Published in final edited form as:
Dev Neurobiol. 2010 September 15; 70(11): 737–750. doi:10.1002/dneu.20807.

Synaptic Drive at Developing Synapses: Transient Up-Regulation of Kainate Receptors

Brigitte van Zundert[1,2,3,*], **Jiang-Ping Zhao**[1], and **Martha Constantine-Paton**[1]

[1]McGovern Institute for Brain Research, Massachusetts Institute of Technology, Cambridge 02139, USA.

[2]Day Laboratory for Neuromuscular Research, Department of Neurology, Massachusetts General Hospital, Harvard Medical School, Boston, MA 02115, USA.

[3]Center for Biomedical Research, Faculty of Biological Sciences and Faculty of Medicine, University Andres Bello, Avenida Republica 217, Santiago, Chile.

Abstract

At the onset of a period of intense synaptic refinement initiated by synchronized eye-opening (EO), rapid changes in post-synaptic NMDA receptor and AMPA receptor currents (NMDARcs, AMPARcs) occur within the superficial visual layers of the rodent superior colliculus (sSC; Lu and Constantine-Paton, 2004). Subsequently, evoked non-NMDARc amplitudes increase, but by 2 weeks after EO (AEO) they decrease significantly. Here, using whole-cell patch-clamp recording, we demonstrate that small, slowly desensitizing excitatory kainate receptor currents (KARcs) are responsible for the rise and subsequent fall in non-NMDARcs. The increase in KAR transmission parallels inhibitory $GABA_A$ responses that plateau at 7 days AEO. By 2 weeks AEO, KARcs are gone. AMPARcs remain unchanged during the appearance and disappearance of the KARcs, despite increases in sSC neuropil activity and continued refinement of inputs to individual sSC neurons. We suggest that in the interval of heightened activity, before SC inhibition matures, many AMPARcs desensitize and are relatively ineffective at relieving the Mg^{2+} block on NMDARs. This transient appearance of slowly desensitizing, long-duration KARcs may provide increased membrane depolarization necessary for NMDAR function and continuation of synaptic refinement.

Keywords

AMPA; NMDA; Kainate; GABA; superior colliculus

INTRODUCTION

It is well established that fast glutamatergic synaptic transmission and its many roles in brain function are mediated by AMPARs and NMDARs. However, mounting evidence indicates that KARs also play important roles in these processes. The modulation of transmitter release by presynaptic KARs and their facilitation of presynaptic forms of short and long term synaptic plasticity has been most extensively studied (Lauri et al., 2007; Lerma, 2006) and, with the advent of ligands that differentiate AMPARs from KARs, postsynaptic KARs have been found in many regions of the central nervous system including the hippocampus, cortex, cerebellum, amygdala, spinal cord, and retina (Castillo et al., 1997; Cossart et al.,

[*]**Corresponding author:** Brigitte van Zundert, Center for Biomedical Research, Faculty of Biological Sciences and Faculty of Medicine, University Andres Bello, Avenida Republica 217, Santiago, Chile. bvanzundert@unab.cl.

1998; Frerking et al., 1998; Kidd and Isaac, 1999, 2001; Bureau et al., 2000; Li and Rogawski, 1998; Li et al., 1999; DeVries and Schwartz, 1999; DeVries, 2000). Many of these receptors produce small, long-decaying and slowly desensitizing currents that are thought to support novel functions at the postsynaptic glutamate synapse. For example, recent data from hippocampal CA3 pyramidal neurons, the cells where these postsynaptic KARs were first described (Castillo et al.,1997; Vignes and Collingridge, 1997), suggest that KARs play an important role in modulating postsynaptic spike frequency by interacting with metabotropic receptors to regulate fast and medium fast after-hyperpolarizing K^+ potentials (Fisahn et al., 2005). Also, simulations of glutamate mediated EPSPs in CA1 interneurons suggest that slowly desensitizing KARs generate tonic depolarizations at synapses where the fast AMPARs do not (Frerking and Ohliger-Frerking, 2002). Such observations have led to the suggestion that the two non-NMDARs ionotropic glutamate receptors encode different temporal information and that KARs may be more important than AMPARs in coincidence detection (Frerking and Ohliger-Frerking, 2002).

Unfortunately, the physiological role of postsynaptic slowly desensitizing KARs in developmental plasticity is still poorly understood largely because most studies pool AMPARs and KARs together as AMPA/KARs or non-NMDARs. However, in the neonatal thalamocortical projection to layer IV of the barrel cortex, postsynaptic KAR-containing synapses predominate. These are later replaced by AMPAR containing synapses (Bannister et al., 2005; Kidd and Isaac, 2001). In addition, Kidd and Isaac (2001) have shown that application of potentiating stimulation applied to this thalamocortical projection results in rapid removal of KAR responses. In this pathway miniature non-NMDARcs are mediated either by KARs or AMPARs, but there is no evidence of both receptors at single active sites.

In the present study we used selective AMPAR and KAR ligands (Cossart et al., 2002) to study the relative contribution of KARs to glutamatergic activity during visual system development resulting from synchronized EO. Eye opening is an important event in visual system development and has been implicated in the reorganization of visual synapses and refinement of axon inputs (Chen and Regehr, 2000; Yoshii et al., 2003; Maffei et al., 2004; Gandhi et al., 2005). Using electrophysiological recordings, we found evidence for refinement of inputs to individual sSC neurons during a 7 day period AEO (Lu and Constantine-Paton, 2004). Thus at 12 hrs, 1 day, 3 days and 7 days AEO there is a progressive reduction in the number of inputs and an enhancement in the number of release sites per input onto individual sSC neurons. There is also a significant increase in miniature AMPAR current frequency and amplitude during the first 12 hours AEO (Lu and Constantine-Paton, 2004). However, after 12 hours, despite the increase in non-NMDAR/NMDAR ratio, the increase in spontaneous activity in the sSC neuropil (Shi et al., 1997), and the increase in refinement of inputs to sSC neurons, the miniature AMPARcs remain stable for at least 2 weeks (Lu and Constantine-Paton, 2004). These observations suggested to us that another glutamate driven current might be involved to facilitate NMDAR dependent ongoing refinement. Here, using a specific AMPAR antagonist to selectively record KARcs and a specific KAR agonist to desensitize KARs and isolate AMPARcs, we show that KAR-mediated transmission increases dramatically between 1 and 7 days AEO and that the KARc increase is coincident with an increase in spontaneous $GABA_A$ receptor currents ($GABA_A$Rcs). We suggest that the transient, slowly-desensitizing, long decay-time KARcs represent a previously unrecognized form of developmental synaptic homeostasis: that they may be responsible for maintaining temporal summation and excitatory drive, allowing NMDAR depolarization at visual sSC synapses during a period where AMPARcs are relatively desensitized because pattern driven visual activity is high and inhibitory transmission has not yet matured.

METHODS

The following data, though not in the same format, have been published previously in Lu and Constantine-Paton (2004), where the EO induced changes in AMPAR and NMDARcs were reported: Number of inputs per neuron up to 7 days AEO (Figure 1C), measurements of the evoked AMPAR component up to 3 days AEO (Figure 5B; black bars), measurements of the miniature AMPARcs up to 3 days AEO (Suppl. Fig. 1). They are included here for comparison with the KAR data that covers a longer AEO interval.

Animal Treatment

Pregnant Sprague-Dawley female rats were purchased and allowed to give birth at MIT so that the day of birth (P0) was accurately ascertained. P10 pups were anesthetized with brief exposure to isoflurane, and both eyelids were sealed with Vetbond (3M) tissue glue. EO (removing the glue and opening the eyelids) was accomplished at 2 times (P12 and P14) and several pups were examined at P19 without eyelid opening. The latter animals showed no KARcs and were not analyzed further. Pups remained with their mother until sacrifice. Midbrain slices from the pups were examined at intervals of 6 hrs, 12 hrs, 1 day, 3 days, 7 days and 14 days AEO. For the preparation of brain slices, pups were anesthetized with isoflurane and decapitated prior to dissection of the midbrain. All procedures followed MIT IACUC-approved protocols.

Electrophysiology

Whole-cell recordings were from neurons of the stratum griseum superficiale (SGS) of the superior colliculus in 350 μm parasaggital sections of the midbrain. Recorded neurons were imaged with infrared differential interference contrast and ranged in soma size from 15 to 20 μm. This size range and location enriched for narrow field vertical neurons but probably also included some piriform cells (Langer and Lund, 1974). Vibratome slices were equilibrated in artificial cerebro-spinal fluid (ACSF) (117 mM NaCl, 4 mM $MgCl_2$, 4 mM KCl, 1.2 mM $NaHPO_4$, 26 mM $NaHCO_3$, 4 mM $CaCl_2$, 20 mM glucose, and 2 μM glycine) for at least 1 hr prior to recording. For all experiments, recording pipettes (5–10 mΩ) were filled with 122.5 mM Cs-gluconate, 17.5 mM CsCl, 8 mM NaCl2, 10 mM HEPES (CsOH), 0.2 mM Na-EGTA, 2 mM Mg-ATP, and 0.3 mM Na-GTP at pH 7.2–7.4. All neurons maintained seal resistances of above 1 GΩ. Series resistances were <40 MΩ, and input resistances were 800–900 MΩ. For evoked recordings, electrical stimuli were delivered to the stratum opticum of the SC through a bipolar stimulating electrode composed of a pair of tungsten microelectrodes (WPI) with tip separation of ~50–100 μm. Recordings used an Axopatch 200B amplifier, a Digidata 1322A interface, and a PC running Axoclamp software. Currents were sampled at 10 kHz and filtered at 5 kHz. Evoked non-NMDA:NMDAR current ratios and subsequent isolated NMDARcs, AMPARcs and KARcs were recorded using single stimuli with intensities that produced amplitudes at approximately 50% saturation for the particular neuron's response. Evoked non-NMDARcs were recorded at −70 mV with $GABA_A$Rs and NMDARs blocked with BMI (10 μM) and D,L-AP5 (50 μM), respectively. Subsequently, APV was washed out and DNQX was added to record isolated evoked NMDARcs at +40 mV. To washout APV, slices were perfused with ~50 ml of ACSF. Given our perfusion rate at 2–2.5 ml/min this took between 20 and 25 minutes. To isolate the evoked KARcs, SYM2206 (40 μM) was also added to the bath.

To obtain the estimated number of inputs per neurons (Figure 1C), minimal stimulation was achieved by gradually increasing the stimulating current from zero until the first evoked currents were observed (2–6 μA). Repetition of this stimulus with either a failure or the same evoked current was considered activation of a single axon. Estimations of the number of inputs converging on a single sSC neuron were made by gradually increasing stimulating

currents. Criteria for distinguishing increases in the evoked currents as a contribution of an additional axon was a clear-cut shoulder on the evoked current rising phase, and the stability of this response to multiple stimuli of the same intensity (Purves and Lichtman, 1985; Chen and Regehr, 2000).

Spontaneous AMPAR miniature currents were recorded at −70 mV with BMI (10 μM), D,L-AP5 (50 μM), SYM2081 (50 μM) and TTX (1 μM) in the bath. For KAR miniature current recordings, BMI (10 μM), D,L-AP5 (50 μM), SYM2206 (10 μM) and TTX (1 μM) were added to the ACSF. Evoked and miniature recordings were made at least 3 minutes after the different antagonists were perfused (rate 2–2.5 ml/min) into the bath unless otherwise stated. Spontaneous $GABA_AR$ currents were recorded at −70 mV with D,L-AP5 (50 μM) and DNQX (10 μM) in the bath.

Data Analysis

Using the Minianalysis 5.1 program, synaptic currents were characterized by the following parameters: peak amplitude, rise-time, and decay-time. Baseline noise ranged from 2.5–5.0 pA peak to peak, and synaptic events with an amplitude 2 times 1/2 peak-to-peak noise were analyzed. Spontaneous events were measured in a total of 75–180 sec of recording from each neuron chosen randomly throughout the recording period. To measure the kinetics of the currents, each synaptic event that was selected was then individually curve fitted (in section “Group analysis and Curve fitting” of Mini Analysis): the rise time was measured form 10%–90% of peak amplitude, while decay-time was fitted from 100%–0% peak amplitude with a single exponential and is given in ms throughout the text as decay interval measured at 0.37 peak amplitude. The same procedure was maintained regardless of the age of the pup contributing the slice. Though this procedure for measuring decay times of small, slow currents like those of native KARs is merely a rough estimate of the actual decay times, it does allow comparisons between the miniature AMPAR and KAR currents, within the same amplitude range, and is therefore used here. The small sizes of the miniature events relative to peak-peak noise levels prohibited a more accurate curve fitting approach although averaging sKARs, mKARs and eKARs (Fig. 5C) showed similar kinetics after scaling.

Drugs

D,L-AP5, BMI and TTX to block NMDARcs, $GABA_ARcs$ and voltage dependent Na^+ channels, respectively, were from Sigma. DNQX, SYM2206, and SYM2081 to block non-NMDAR glutamate currents, AMPARcs, and desensitize KARcs, respectively, were from Tocris.

Statistical Analyses

A two-tailed ANOVA followed by the Tukey post hoc test was used to detect intervals in which significant changes occurred for all data sets where a parameter was measured across ages within a treatment. Non-parametric Kolmogorov-Smirnov and Mann-Whitney tests were used to test for significance of pooled current parameters when either AMPARcs or KARcs were removed from non-NMDAR current recordings.

RESULTS

Evoked, spontaneous, and miniature whole-cell recordings were obtained from the superficial visual layers of the sSC before eye opening (BEO), AEO, and in several animals maintained with EO until P19. This eyelid-opening paradigm synchronizes vision-driven changes in the visual pathway and greatly facilitates analyses of the effects of EO on synaptic refinement and development of excitatory and inhibitory currents. Rat pup EO was performed on P12 and P14 (normal EO is at P13) in this study.

Non-NMDARcs increase during input elimination then show a significant drop from 7 to 14 days AEO

Earlier we demonstrated that isolated AMPARcs increase in frequency and amplitude within the first day AEO (Lu and Constantine-Paton, 2004). Here we show that an increase in non-NMDARcs continued until 7 days AEO regardless of whether eyes were opened on P12 (Fig. 1A) or P14 (Fig. 1B). sSC neurons from P12 EO pups were subsequently studied at 2 weeks AEO and the increase in non-NMDARcs dropped to the same number as observed at 3 days AEO (Fig. 1A). In the same interval (3 days and 2 weeks AEO); refinement in the number of inputs on sSC neurons continued to decrease (Fig. 1C bottom) and AMPAR mEPSC amplitude and frequency remained stable (Suppl. Fig. 1). Consequently, we asked if changes in the small slow KARcs, first detected in our earlier study (Lu and Constantine-Paton, 2004), were responsible for the rise and subsequent fall of the non-NMDAR current and might therefore facilitate continuing depolarization needed to activate NMDARs during the prolonged refinement of sSC circuitry.

Two kinetically different non-NMDAR excitatory miniature currents are prominent 3 to 7 days AEO

Small miniature non-NMDARcs with slow decay kinetics became frequent in sSC recordings with TTX, APV, and BMI at 3 days AEO (see * in Figure 2A) in all neurons from which low noise recordings were obtained. In addition to the small slow currents, we also observed some large fast onset currents with slow decays (see #, Fig.2A) along with large, fast, presumably pure AMPARcs (Fig. 2A; currents not indicated with a symbol). However, by 14 days AEO (P26), only fast currents remained in these recordings. Scatter plots of amplitude *versus* decay-time (Fig. 2B) and of decay-time *versus* rise-time (Fig. 2C) from 3 typical sSC neurons at 1, 7 and 14 days AEO are plotted for all the quantal non-NMDAR glutamate currents occurring within a randomly chosen 3 minutes of recording. The kinetics of the non-NMDA mEPSCs recorded at 1 and 14 days AEO were similar: Peak amplitudes ranged up to 25 pA with fast decay-times (0.1–7 ms) and rise-times (0.1–5 ms). By contrast, non-NMDAR mEPSCs recorded at 7 days AEO (middle panels) showed an additional population of events with decay-times ranging from 7 to 20 ms, rise-times from 5 to 15 ms, and peak amplitudes mostly in the range of 6–15 pA. In addition to the isolated small currents, some larger, fast rise-time currents, initially assumed to be pure AMPAR mediated quantal events, also showed increased decay-times. One of these events can be seen in the current trace shown for 7 days after AEO (Fig. 2A,#) and similar currents can be identified by their kinetics in the scatter plots of quantal events from a typical 7 days AEO sSC neuron (middle panels Fig. 2B,C). Few, if any, small slow mEPSCs were detected BEO, at 24 hours AEO and at 14 days AEO (Fig. 2A,B,C).

The age-dependent heterogeneity in the non-NMDAR currents was obvious in summary graphs of their averaged miniature current amplitude (Fig. 2D, left) and frequency (Fig. 2D, right) recorded in P11 to P26 sSC. The mixture of large and small quantal events seen in all recorded neurons at 7 days AEO are consistent with the smaller average amplitude of the miniature non-NMDARcs seen in Figure 2D (left) at the same time point. The peak in average non-NMDAR miniature current frequency at 7 days AEO is also consistent with the transient appearance of these small miniature currents (Fig. 2D, right). Taken together, the current data indicates a peak in non-NMDAR:NMDAR excitatory current ratios at 7 days (Fig. 1), while AMPARcs (Suppl. Fig 1) remain relatively constant, and suggests that the slow mEPSCs reported here reflect the third ionotropic glutamate receptor. These transient KAR's are responsible for the peak in evoked current ratios at 7 days AEO and for the significant drop in the non-NMDAR currents at P26, 2weeks AEO (Fig. 5B). We next used a KAR-specific ligand to determine whether the small slow currents were KARcs and the extent they could contribute significantly to non-NMDAR excitatory events.

Transiently appearing small slow currents are KARcs

To eliminate AMPAR mediated miniature currents from the non-NMDAR quantal events we applied the specific AMPAR current antagonist SYM2206 (10 μM) at 7 days AEO to the bath containing Mg^{2+}, TTX, APV and BMI. Figure 3A illustrates typical traces from one neuron with continuous SYM2206 exposure. During SYM2206 application the largest currents with faster decay-time and rise-time disappeared into the noise level, leaving smaller mEPSCs with slow kinetics. As can be seen in Figure 3B,C by comparing the control and SYM2206 scatter plots of two separate neurons for amplitude *versus* decay-time (left column), and decay-time *versus* rise-time (right column), SYM2206 reduced a population of events with large amplitudes (>15 pA), fast decay-times (<3.5 ms) and fast rise-times (<2 ms). Similar findings were obtained from all 5 neurons where the SYM2206 application was successfully completed as shown in the pooled data summary histograms and cumulative probability plots of Figure 3D–F (thin line before, and broad line after, SYM2206 application in insets). The remaining mEPSCs are similar to the slowly desensitizing postsynaptic KARcs reported by previous investigators (Castillo et al., 1997; Kidd and Isaac, 1999; Bannister et al., 2005) and most closely match the KARc decay times recorded in the small CA1 inhibitory neurons by Cossart et al., (2002).

To specifically remove KARcs from non-NMDAR quantal events of 7 days AEO SC neurons, we used desensitization with the specific KAR agonist SYM2081, as we were unable to obtain GYK152466 (Cossart et al., 2002). SYM2081, after a long application, selectively desensitizes and eliminates KARcs from recordings (Savidge et al. 1999; Cossart et al., 2002). Our mEPSC recordings confirm that SYM2081 activates postsynaptic KARs after a short perfusion (4–10 min; Fig. 4A,B). However, after 15 minutes of perfusion with SYM2081 only fast currents remained. This can be seen in the pooled data, summary histograms, and cumulative probability curves of Figure 4C–E obtained from the 4 neurons analyzed. The fact that the cumulative probability curves of amplitude for control and SYM2018 neurons do not show a significant difference suggests the presence of mixed AMPARcs/KARcs in which their amplitude is mainly defined by the large AMPARc. These data provide pharmacological evidence that the other component of the non-NMDARs glutamate activity in the sSC is mediated by postsynaptic KARcs.

KARcs are responsible for the transient increase in evoked non-NMDARcs between 3 to 7 days AEO

To accurately determine the contribution of KARs to evoked non-NMDAR:NMDAR current ratios at successive times AEO, we examined evoked non-NMDAR EPSCs at −70 mV as in Figure 1A–B, except that recordings were made before (green line) and after (red line) blockade of AMPARs with SYM2206 (Fig. 5A). Evoked non-NMDAR:NMDAR current amplitude ratios were taken from at least 6 neurons in several slices at 1 day BEO (P12), and at 6, 12, 24 hrs and 3, 7, and 14 days AEO (Fig. 5B). As can be seen in the histogram of Figure 5B by the black bars, between 12 hours and 24 hrs AEO evoked AMPARcs showed the potentiation described previously (Lu and Constantine-Paton, 2004) and then remained unchanged till 14 days AEO. In contrast, the red bars show that the contribution of the evoked KAR current increased most rapidly between 3 and 7 days AEO. Remarkably, at 7 days AEO this evoked KAR current contribution constituted 45% of the total non-NMDAR response. At 14 days AEO (P26), the KAR current contribution was gone and the evoked AMPAR current amplitude that remained was not significantly different from the evoked AMPAR current at 24 hrs AEO. Taken together, the miniature current data and the evoked current data indicate that the increases in non-NMDAR:NMDAR current ratios, are due to the addition of KARs and not AMPARs to the sSC synapses between 1 day and 7 days AEO.

Evoked and miniature KARcs have the same kinetics

Our recordings of the spontaneous, miniature and evoked non-NMDA currents all suggest that KARs, in addition to or rather than AMPARs, are involved in the refinement of axonal projections targeting sSC neurons between 1 day and 7 days AEO. We scaled sKAR, mKAR and eKARcs to determine if all showed the same kinetics. In sSC neurons studied at 7 days AEO, KAR were isolated with BMI, APV and SYM2206 and the evoked events were averaged in the absence and then in the presence of TTX. After scaling it can be observed that the spontaneous (black line), miniature (green line) and evoked (red line) KARcs have similar rise-times and decay-times (Fig. 5C).

Transient increase in evoked KAR current at 3–7 days AEO parallels increases of GABAergic transmission

Earlier whole cell patch-clamp recordings in the sSC documented that GABA mediated inhibition is already established in the rodent sSC at the time of birth (Jüttner et al., 2001) and our own previous studies suggested that inhibitory $GABA_AR$ currents begin to exert a suppressing effect on spontaneous EPSCs around P18-19 (Shi et al., 1997; Aamodt et al., 2000). This was temporally associated with an up-regulation of the GABA transporters (Shi et al., 1997). Thus a possible association between $GABA_AR$ differentiation and the KAR current peak prompted us to examine changes in $GABA_AR$ currents using the P12 controlled EO paradigm. Spontaneous $GABA_AR$ currents were isolated in ACSF containing APV and DNQX and recorded at −70 mV. Figure 6A shows traces of GABAergic activity at 7 days AEO. Both the averaged $GABA_AR$ current amplitude and averaged frequency exhibited their greatest increase in the AEO interval between 3 and 7 days AEO (Fig. 6B–C). $GABA_AR$ currents appeared to plateau around 7 days AEO because, at 14 days AEO, $GABA_AR$ current amplitude and frequency were identical to those observed a week earlier. Therefore, the development of the GABAergic transmission correlates with the maturation of the KAR-mediated currents (Fig. 5B) suggesting that KARcs are potentially involved in this final stage of inhibitory circuitry development in the sSC.

DISCUSSION

The goal of this study was to identify further changes in the function of ionotropic glutamate receptors during development using controlled eyelid opening to initiate a period where synaptic refinement is ongoing, where significant changes in NMDARs and AMPARs are no longer occurring, but where non-NMDAR glutamate currents are changing rapidly (Lu and Constantine-Paton, 2004). Recordings from large (~ 15–20 μm) neurons in the SGS of the sSC the small postsynaptic excitatory currents we focus on here were found in every neuron where stable whole cell recordings allowed sufficient examination of small synaptic events. We show that post-synaptic KARs are responsible for these transient currents and that they disappear from recordings by 2 weeks AOE.

In the visual layers of the rodent sSC AEO, all cells have already established a robust, topographically refined innervation from the retina (Simon and O'Leary, 1992). The dense visual cortical projection is arborizing and refining in the sSC at this time (Phillips et al., in preparation) and excitatory activity within the sSC is increasing (Shi et al., 1997). KAR mediated responses beginning between 1 and 3 days AEO, regardless of EO day, were highly predictable and transient across all slices examined, and they therefore reflect a novel, and potentially important aspect of glutamate synaptogenesis. KARcs peak in frequency and in contribution to the non-NMDAR current evoked response at 7 days AEO. At this time they are responsible for nearly 50% of the evoked non-NMDAR:NMDAR current ratio (Fig. 5B): an increase which was originally attributed to an increase in AMPAR responses because we were using the non-selective antagonist NBQX. Throughout, the small

non-NMDAR currents display low peak amplitudes, long decay-times, and low levels of desensitization: properties first described for postsynaptic KARcs in CA3 pyramidal neurons after mossy fiber stimulation (Castillo et al., 1997; Vignes and Collingridge, 1997) and, most significantly, these small, slow currents remained in the presence of the specific AMPAR antagonist SYM2206 but were desensitized after long exposure to the specific KAR agonist SYM2081. During the entire AEO period when KARcs are present, the amplitude of the evoked and miniature AMPARcs does not change (Fig. 5B, Suppl. Fig. 1). Therefore, the significant drop in the non-NMDAR:NMDAR evoked current ratio between 7 and 14 days AEO appears to be due entirely to the loss of KARcs. We postulate that their earlier appearance may represent a heretofore unrecognized homeostatic mechanism to maintain NMDAR function when AMPAR function is likely to be depressed. This idea is motivated by our additional finding that the increase in KARcs is paralleled by an AEO increase in $GABA_A$ inhibitory currents that plateau at 7 days AEO and disappear in the next week. We elaborate on this hypothesis below after reviewing relevant earlier work on postsynaptic KARs.

An important initial question is whether the increases in the small, slowly desensitizing KARcs are directly causing the AEO increase in inhibition. This is possible because KARs have previously been documented in hippocampal CA1 inhibitory neurons (Cossart, et al., 1998) and there are many inhibitory interneurons in the sSC. However, this possibility does not explain the present observations because a KAR activity-induced increase would not account for the disappearance of KARcs with age and the idea would require that all the relatively large neurons we recorded from in our experiments were inhibitory. The latter is unlikely because most of these larger sSC neurons express CAMKII (Phillips, M personnel communication), a kinase believed to be restricted to excitatory cells (Jones et al., 1994).

In contrast, several lines of evidence suggest our opposite interpretation: that KARs appear *because of* the late development of inhibition in the sSC AEO. Electrophysiological experiments and computer simulations indicate that the KAR contribution to synaptic transmission relative to the AMPAR component is underestimated in EPSC recordings: the technique that we and others generally use to study small synaptic events. However, it is EPSPs that drive neurons *in vivo* and the KAR component of the EPSP is predicted to show pronounced tonic, temporal summation at input frequencies between 50–100 Hz (Frerking and Ohliger-Frerking, 2002). The frequencies of postsynaptic excitatory events are much lower in acute slices then they are in the intact brain, but *in vivo* microelecrode recording from the sSC in rats with fully developed inhibitory circuits show responses to moving or changing visual stimuli occurring at well over 50 Hz (Girman and Lund, 2007). This supports an assumption critical to our hypothesis: namely, that the slowly desensitizing KARcs could produce sufficient depolarization to compensate for AMPAR desensitization and failure to remove the magnesium block on NMDAR current. This AMPAR desensitization is likely to be most pronounced AEO when collicular activity is high (Shi et al., 1997), because pattern vision starts driving and maturing the visual pathway, but before inhibitory circuitry is able to downregulate ongoing excitation. This is the same period when the very slowly desensitizing KARc contributions to synaptic depolarizations are high and potentially capable of enabling continued NMDAR activation for the ongoing synaptic refinement, potentiation, and stabilization, that we know is occurring (Lu and Constantine-Paton, 2004; Zhao et al., 2006).

Transient postsynaptic KARc involvement in neural development was first described in the neonate thalamic projection to the barrel cortex of rats (Kidd and Isaac, 1999). In this pathway the KAR contribution to spontaneous events decreased during the first postnatal week, the period of maximum plasticity in barrel cortex, while the AMPARcs increased. In addition, pairing-induced LTP in this pathway caused a rapid reduction in the KAR

component as AMPARcs increase even though the KARcs and AMPARcs never arose from the same active sites in the barrel cortex patch clamp recording (Bannister et al., 2005). The transient KARs we describe in the present study differ in several respects from those in the neonate barrel cortex. First, they appear in the sSC at a later stage of development, the 2nd to 3rd postnatal weeks as compared to the 2nd to 4th postnatal days in the barrel cortex. Second, in the sSC AMPAR addition to synapses has already occurred within 24 hrs hours AEO (Lu and Constantine-Paton, 2004; Zhao et al., 2006; Suppl. Fig.1), before KARcs appear. Third, combined AMPA/KARs are occasionally observed in the sSC suggesting that KAR responses don't reflect the simple switch of KAR synapses for AMPAR synapses as suggested by the barrel cortex work. Fourth, unlike this sSC study (Fig. 6), there is no reported increase in the barrel cortex spontaneous inhibitory $GABA_A$ currents when early KARcs are present (Daw et al., 2007). Hyperpolarizing $GABA_A$ currents are present in the rat sSC as early as P1 (Jüttner et al., 2001), but the AEO increase in GABA currents is correlated with a large increase in the expression of glutamic acid dehydrogenase (GAD), the synthetic enzyme for GABA, and with an upregulation GABA transporters GAT-1 and GAT-2 (Shi et al., 1997), indicating that the maturation of sSC inhibitory transmission occurs at this much later stage and probably operates to control and decrease AEO increases in activity (Shi et al., 1997). In the barrel cortex no pronounced changes in inhibition are occurring when KARs predominate at neonate thalamocortical synapses. Nevertheless there are also few AMPARs at these synapses since they only appear and replace KARs when NMDAR dependent-LTP is experimentally induced by pairing. In the young barrel cortex input refinement is occurring when KARcs are first observed. NMDAR function is required during this period as been established by barrel neuron dendritic disorganization in a conditional KO of layer 4 NR1 (Iwasato et al., 2000). Thus, the presence of KARcs in the target neurons of the neonate barrel cortex and sSC at the onset of pattern vision may be fulfilling the same function: that of driving the NMDAR current.

To test the hypothesis that the KARcs represent a homeostatic response to low levels of ionotropic glutamate current at a time when depolarization is needed to produce required NMDAR function would be facilitated if the KAR subunits involved were identified. KARs are tetramers and can contain any of 5 different subunits. Of these 5 subunits, GluR6 and KA2 have been shown to bind the glutamate receptor scaffold, the membrane associated guanylate kinase (MAGUK) PSD-95 (Garcia et al., 1998; Mehta et al., 2001). GluR6 binds to a PDZ domain of PSD-95 and KA2 binds to the SH3 and GK domains of PSD-95. This is potentially significant to the visual pathway studied here because PSD-95 is the dominant postsynaptic density MAGUK at sSC neuron synapses during the 7 day AEO period (Yoshii et al., 2003) when postsynaptic KARcs are obvious in our recordings. Indeed Garcia et al., (1998) report that it is this binding to PSD-95 that endows KARs with the incomplete desensitization seen in neuronal postsynaptic KARs by us and others. This incomplete desensitization has not been reported upon heterologous expression of KARs (Herb et al., 1992). We have not investigated KAR subunits in the sSC. However, Mulle et al., (1998) show that the postsynaptic KARcs in hippocampal CA3 pyramids are virtually undetectable in the GluR6 −/− mouse, but are not perturbed in the GluR5−/− mouse. Also, in CA3 KA2−/− mice postsynaptic KARs appear normal (Contractor et al., 2003). Such results suggest that the GluR6 subunit may be a prominent component of the postsynaptic sSC KARs reported here.

The KAR subunits responsible for the transient post-synaptic appearance of KARcs in maturing sSC neurons need to be identified before hypotheses concerning the function of these currents can be tested. However, their transient appearance in the narrow window after EO when inputs to visual collicular neurons are still refining, but when NMDAR function might otherwise be low due to AMPAR desensitization, together with the earlier appearance of KARs in the neonate barrel cortex before AMPARs are upregulated, suggests that this

third type of ionotropic glutamate receptor may have previously unrecognized functions during brain development. In this respect it is intriguing that reduced NMDAR function is associated with the symptoms of schizophrenia both in people and in rodents (Javitt and Zukin, 1991; Lahti et al., 1995); some post mortem studies in human schizophrenics have reported decreases in KAR receptor binding, and abnormal polymorphisms in SNPS for KAR genes GRIK3 and GRIK4 have been associated with schizophrenics in several human studies (Pikard et al., 2008; Kahler et al., 2009). Moreover, a recent report (Duncan et al., 2010) implicates greatly increased sensitivity to KAR agonists in transgenic mice with reduced NMDAR function. Evidence for defects in post- *versus* pre-synaptic localization of KARs is absent in such studies. However, such reports suggest further exploration of possible stimulation of postsynaptic KAR function in situations of low NMDAR activity and may prove critically informative for understanding brain circuit function both in normal development and in crippling psychiatric disease.

Supplementary Material

Refer to Web version on PubMed Central for supplementary material.

Acknowledgments

Supported by NIH EY01407 (M.C-P), The Pierre L. de Bourknecht ALS Research Fund (B.v.Z) and Fondecyts 1070494 and 1101012 (B.v.Z). We acknowledge the contribution of Dr. Wei Lu then a member of the MCP laboratory to the initial discovery of KARcs.

REFERENCES

Aamodt SM, Shi J, Colonnese MT, Veras W, Constantine-Paton M. Chronic NMDA exposure accelerates development of GABAergic inhibition in the superior colliculus. J Neurophysiol. 2000; 83:1580–1591. [PubMed: 10712481]

Bannister NJ, Benke TA, Mellor J, Scott H, Gurdal E, Crabtree JW, Isaac JT. Developmental changes in AMPA and kainate receptor-mediated quantal transmission at thalamocortical synapses in the barrel cortex. J Neurosci. 2005; 25:5259–5271. [PubMed: 15917466]

Bureau I, Dieudonne S, Coussen F, Mulle C. Kainate receptor-mediated synaptic currents in cerebellar Golgi cells are not shaped by diffusion of glutamate. Proc Natl Acad Sci USA. 2000; 97:6838–6843. [PubMed: 10841579]

Castillo PE, Malenka RC, Nicoll RA. Kainate receptors mediate a slow postsynaptic current in hippocampal CA3 neurons. Nature. 1997; 388:182–186. [PubMed: 9217159]

Chen C, Regehr WG. Developmental Remodeling of the Retinogeniculate Synapse. Neuron. 2000; 28:955–966. [PubMed: 11163279]

Contractor A, Sailer AW, Darstein M, Maron C, Xu J, Swanson GT, Heinemann SF. Loss of kainate receptor-mediated heterosynaptic facilitation of mossy-fiber synapses in KA2−/− mice. J Neurosci. 2003; 23:422–429. [PubMed: 12533602]

Cossart R, Epsztein J, Tyzio R, Becq H, Hirsch J, Ben-Ari Y, Crepel V. Quantal release of glutamate generates pure kainate and mixed AMPA/kainate EPSCs in hippocampal neurons. Neuron. 2002; 35:147–159. [PubMed: 12123615]

Cossart R, Esclapez M, Hirsch JC, Bernard C, Ben-Ari Y. GluR5 kainate receptor activation in interneurons increases tonic inhibition of pyramidal cells. Nat Neurosci. 1998; 1:470–478. [PubMed: 10196544]

Daw MI, Ashby MC, Isaac JT. Coordinated developmental recruitment of latent fast spiking interneurons in layer IV barrel cortex. Nat Neurosci. 2007; 10:453–461. [PubMed: 17351636]

DeVries SH. Bipolar cells use kainate and AMPA receptors to filter visual information into separate channels. Neuron. 2000; 28:847–856. [PubMed: 11163271]

DeVries SH, Schwartz EA. Kainate receptors mediate synaptic transmission between cones and 'Off' bipolar cells in a mammalian retina. Nature. 1999; 397:157–160. [PubMed: 9923677]

Duncan GE, Inada K, Koller BH, Moy SS. Increased sensitivity to kainic acid in a genetic model of reduced NMDA receptor function. Brain Res. 2010; 1307:166–176. [PubMed: 19840778]

Frerking M, Malenka RC, Nicoll RA. Synaptic activation of kainate receptors on hippocampal interneurons. Nat Neurosci. 1998; 6:479–486. [PubMed: 10196545]

Frerking M, Ohliger-Frerking P. AMPA receptors and kainate receptors encode different features of afferent activity. J Neurosci. 2002; 22:7434–7443. [PubMed: 12196565]

Fisahn A, Heinemann SF, McBain CJ. The kainate receptor subunit GluR6 mediates metabotropic regulation of the slow and medium AHP currents in mouse hippocampal neurones. J Physiol. 2005; 562:199–203. [PubMed: 15539395]

Gandhi SP, Cang J, Stryker MP. An eye-opening experience. Nat Neurosci. 2005; 8:9–10. [PubMed: 15622410]

Garcia EP, Mehta S, Blair LA, Wells DG, Shang J, Fukushima T, Fallon JR, Garner CC, Marshall J. SAP90 binds and clusters kainate receptors causing incomplete desensitization. Neuron. 1998; 21:727–739. [PubMed: 9808460]

Girman SV, Lund RD. Most superficial sublamina of rat superior colliculus: neuronal response properties and correlates with perceptual figure-ground segregation. J Neurophysiol. 2007; 98:161–177. [PubMed: 17475720]

Herb A, Burnashev N, Werner P, Sakmann B, Wisden W, Seeburg PH. The KA-2 subunit of excitatory amino acid receptors shows widespread expression in brain and forms ion channels with distantly related subunits. Neuron. 1992; 8:775–785. [PubMed: 1373632]

Iwasato T, Datwani A, Wolf AM, Nishiyama H, Taguchi Y, Tonegawa S, Knopfel T, Erzurumlu R, Itohara S. Cortex-restricted disruption of NMDAR1 impairs neuronal patterns in barrel cortex. Nature. 2000; 406:726–731. [PubMed: 10963597]

Javitt DC, Zukin SR. Recent advances in the phencyclidine model of schizophrenia. Am J Psychiatry. 1991; 148:1301–1308. [PubMed: 1654746]

Jones EG, Huntley GW, Benson DL. Alpha calcium/calmodulin-dependent protein kinase II selectively expressed in a subpopulation of excitatory neurons in monkey sensory-motor cortex: comparison with GAD-67 expression. J Neurosci. 1994; 14:611–629. [PubMed: 8301355]

Jüttner R, Henneberger C, Grantyn R, Rothe T. Early onset of glutamatergic and GABAergic synaptic activity in the visual layers of the rodent superior colliculus. Int J Dev Neurosci. 2001; 19:255–261. [PubMed: 11337194]

Kahler DS, Jonsson EG, Agartz I, Le Hellard s, Hall H, Jakobsen KD, Hansen T, Melle I, Werge T, Steen VM, Andreassen OA. A possible association between schizophrenia and GRIK3 polymorphisms in a multicenter sample of Scandinavian origin (SCOPE). Schizophrenia Res. 2009; 107:242–248.

Kidd FL, Isaac JT. Developmental and activity-dependent regulation of kainate receptors at thalamocortical synapses. Nature. 1999; 400:569–573. [PubMed: 10448859]

Kidd FL, Isaac JT. Kinetics and activation of postsynaptic kainate receptors at thalamocortical synapses: role of glutamate clearance. J Neurophysiol. 2001; 86:1139–1148. [PubMed: 11535664]

Kim MJ, Futai K, Jo J, Hayashi Y, Cho K, Sheng M. Synaptic accumulation of PSD-95 and synaptic function regulated by phosphorylation of serine-295 of PSD-95. Neuron. 2007; 56:488–502. [PubMed: 17988632]

Lahti AC, Koffel B, Laporte D, Tamminga CA. Subanesthetic doses of ketamine stimulate psychosis in schizophrenia. Neuropsychopharmacology. 1995; 13:9–19. [PubMed: 8526975]

Langer TP, Lund RD. The upper layers of the superior colliculus of the rat: a Golgi study. J Comp Neurol. 1974; 158:418–435. [PubMed: 4615112]

Lauri SE, Palmer M, Segerstrale M, Vesikansa A, Taira T, Collingridge GL. Presynaptic mechanisms involved in the expression of STP and LTP at CA1 synapses in the hippocampus. Neuropharmacology. 2007; 52:1–11. [PubMed: 16919682]

Lerma J. Kainate receptor physiology. Curr Opin Pharmacol. 2006; 6:89–97. [PubMed: 16361114]

Li H, Rogawski MA. GluR5 kainate receptor mediated synaptic transmission in rat basolateral amygdala in vitro. Neuropharmacology. 1998; 37:1279–1286. [PubMed: 9849665]

Li P, Wilding TJ, Kim SJ, Calejesan AA, Huettner JE, Zhuo M. Kainate-receptor-mediated sensory synaptic transmission in mammalian spinal cord. Nature. 1999; 397:161–164. [PubMed: 9923678]

Lu W, Constantine-Paton M. Eye opening rapidly induces synaptic potentiation and refinement. Neuron. 2004; 22:237–249. [PubMed: 15260959]

Maffei A, Nelson SB, Turrigiano GG. Selective reconfiguration of layer 4 visual cortical circuitry by visual deprivation. Nat Neurosci. 2004; 7:1353–1359. [PubMed: 15543139]

Mehta S, Wu H, Garner CC, Marshall J. Molecular mechanisms regulating the differential association of kainate receptor subunits with SAP90/PSD-95 and SAP97. J Biol Chem. 2001; 276:16092–16099. [PubMed: 11279111]

Mulle C, Sailer A, Pérez-Otaño I, Dickinson-Anson H, Castillo PE, Bureau I, Maron C, Gage FH, Mann JR, Bettler B, Heinemann SF. Altered synaptic physiology and reduced susceptibility to kainate-induced seizures in GluR6-deficient mice. Nature. 1998; 392:601. [PubMed: 9580260]

Pickard BS, Knight HM, Hamilton RS, Soares DC, Walker R, Boyd JK, Machell J, Maclean A, McGhee KA, Condie A, Porteous DJ, St Clair D, Davis I, Blackwood DH, Muir WJ. A common variant in the 3'UTR of the GRIK4 glutamate receptor gene affects transcript abundance and protects against bipolar disorder. Proc Natl Acad Sci U S A. 2008; 105:14940–14945. [PubMed: 18824690]

Purves, D.; Lichtman, JW. Principles of Neural Development. Sunderland: Sinaur Associates MA; 1985.

Savidge JR, Sturgess NC, Bristow DR, Lock EA. Characterization of kainate receptor mediated whole-cell currents in rat cultured cerebellar granule cells. Neuropharmacology. 1999; 38:375–382. [PubMed: 10219975]

Simon DK, O'Leary DD. Development of topographic order in the mammalian retinocollicular projection. J Neurosci. 1992; 12:1212–1232. [PubMed: 1313491]

Shi J, Aamodt SM, Constantine-Paton M. Temporal correlations between functional and molecular changes in NMDA receptors and GABA neurotransmission in the superior colliculus. J Neurosci. 1997; 17:6264–6276. [PubMed: 9236237]

Vignes M, Collingridge GL. The synaptic activation of kainate receptors. Nature. 1997; 388:179–182. [PubMed: 9217158]

Yoshii A, Sheng MH, Constantine-Paton M. Eye opening induces a rapid dendritic localization of PSD-95 in central visual neurons. Proc Natl Acad Sci USA. 2003; 100:1334–1339. [PubMed: 12552131]

Zhao JP, Phillips MA, Constantine-Paton M. Long-term potentiation in the juvenile superior colliculus requires simultaneous activation of NMDA receptors and L-type Ca^{2+} channels and reflects addition of newly functional synapses. J Neurosci. 2006; 26:12647–12655. [PubMed: 17151267]

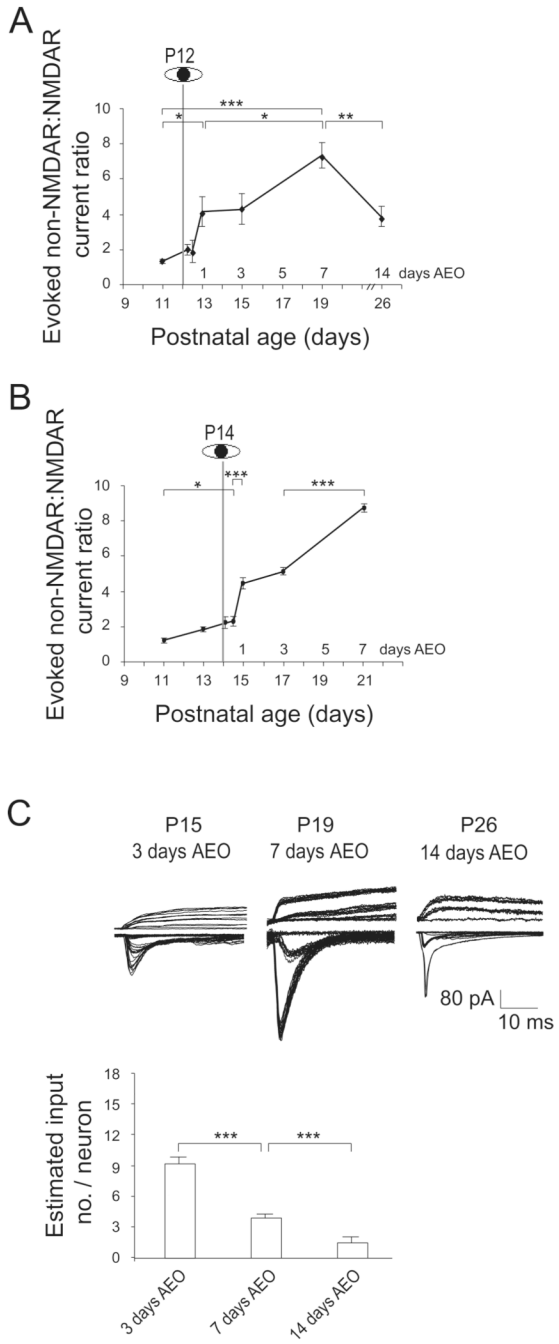

Figure 1.

Non-NMDAR:NMDAR current ratios increase until 7 days AEO, and are associated with major refinement of inputs to sSC neurons. A–B: Quantitative changes in non-NMDAR:NMDAR current ratio relative to the time AEO at P12 (A) and at P14 (B). With EO at either age, non-NMDAR:NMDAR current ratios increased until 7 days AEO. C: Traces illustrate multiple steps of evoked non-NMDARs (eAMPA/KAR) currents (inward) and NMDAR currents (outward) AEO. The method of shoulders was used to estimate the number of inputs per postsynaptic neuron, and indicated a major input elimination between P3 and P7 days AEO. This was followed by a slower decline the subsequent week until only ~1–2 inputs per neuron remained at 14 days AEO (P26). Data for all graphs represent the

mean ± S.E.M. obtained from 7–12 neurons. For clarity, significance for the statistical data is shown only for the two closest and most important time points. For more details see Suppl. Table 1 (Fig. 1A) and Suppl. Table 2 (Fig. 1B).

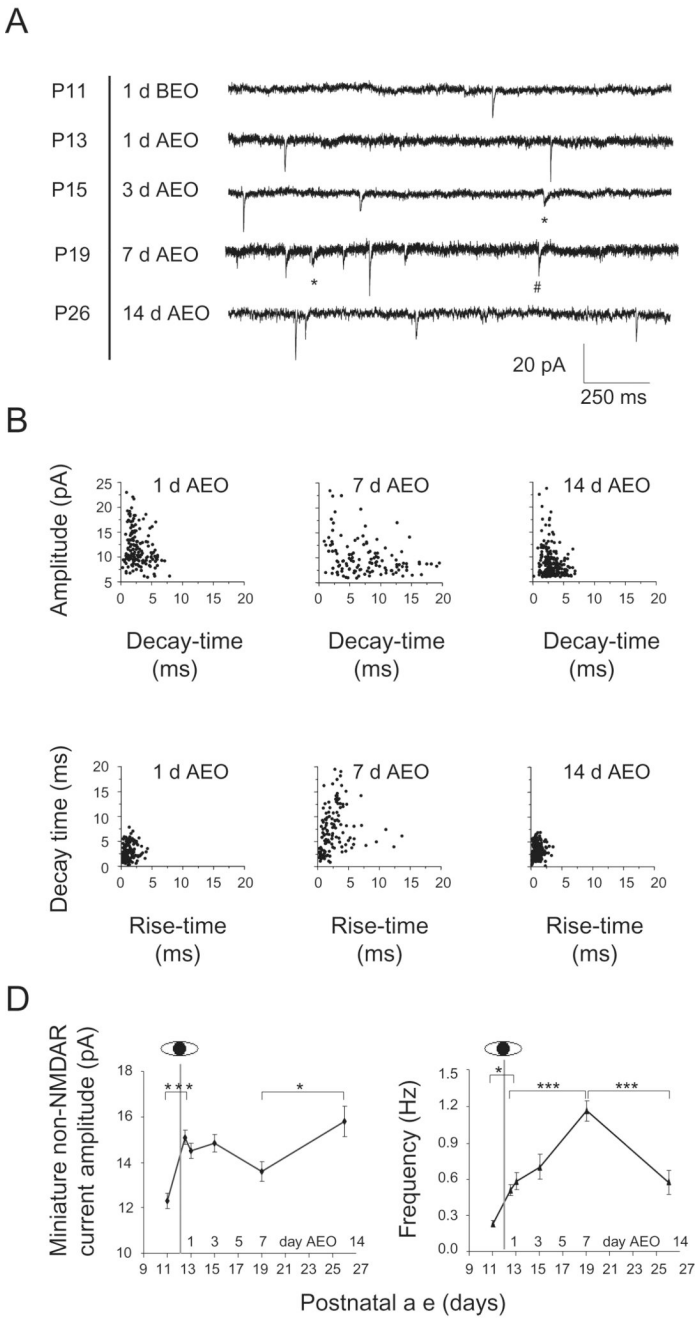

Figure 2.

Emergence of small, slow, non-NMDAR mEPSCs AEO. A: Representative traces show miniature non-NMDAR excitatory currents recorded BEO and AEO with neurons held at −70 mV. From 3 days AEO (P15) to 7 days AEO a population of slowly decaying and small amplitude mEPSCs (*) were detected in addition to the bigger currents that were observed throughout the period of study. Some slow currents with larger amplitudes were also present (#). Slow currents were no longer detectable at 14 days AEO (P26). B–C: Scatter plots of amplitude *versus* decay-time (B) and of decay-time *versus* rise-time (C) from all miniature non-NMDAR current events (n=150–200) in 3 minute sequences chosen at random from recording individual cells at 1 (P13, left), 7 (P19, middle) and 14 (P26, right) days AEO.

Note that in contrast to 1 and 14 days AEO, neurons at 7 days AEO also display a population of mEPSCs with small amplitudes, slow decay-times, and slow rise-times. D: Summary of quantitative changes in average non-NMDAR mEPSC amplitude (left) and frequency (right) relative to the time AEO. Note that at 7 days AEO the average amplitude of the miniature non-NMDAR-EPSCs decreased, whereas their average frequency peaked at this time of development. These changes at P19 are most likely due to the transient appearance of the small slow currents observed at 7 days AEO (see Fig. 2B middle panel). Each symbol represents mean ± S.E.M. obtained from 6–8 neurons. For clarity, significance for the statistical data is shown only for the two closest and most important time points. For more details see Suppl. Table 3 (Fig. 2D, left) and Suppl. Table 4 (Fig. 2D, right).

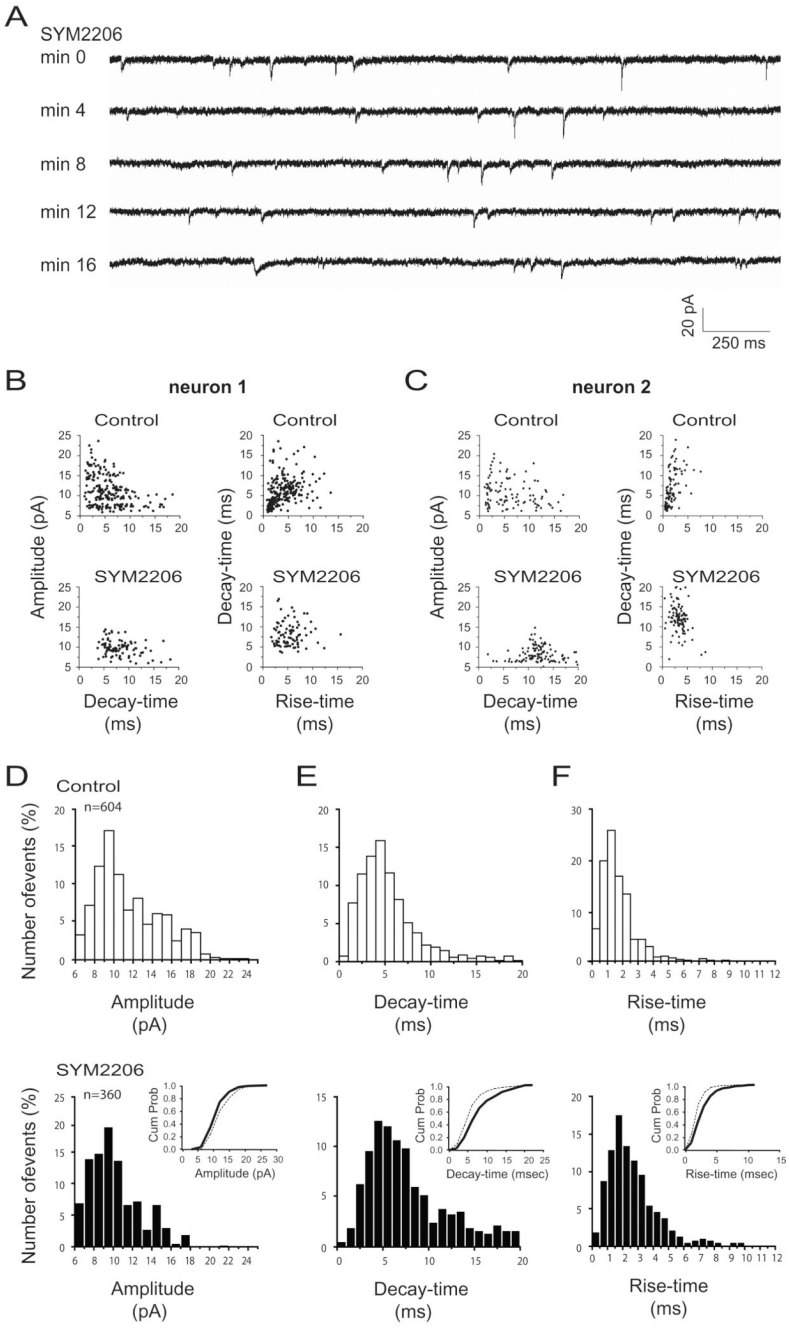

Figure 3.

The smaller and slower non-NMDAR mEPSCs are isolated by the specific AMPAR antagonist SYM2206. A: Representative traces show miniature non-NMDARcs recorded at 7 days AEO. Neurons were held at −70 mV. In addition, neurons were perfused with SYM2206 (10 μm). During SYM2206 application, larger currents with faster decay- and rise-times disappeared into the noise level, leaving, after 16 min of SYM2206 application, smaller mEPSCs with slow kinetics. B–C: Scatter plots of currents from two different neurons showing amplitude *versus* decay-time (left) and decay-time *versus* rise-time (right) of all miniature non-NMDARcs recorded in these neurons for 3 minutes under control conditions (upper panels) and after 15 min exposure of SYM2206 (lower panels). Summary

frequency histograms from the pooled data of all 5 neurons studied showing the parameters amplitude (D), decay-time (E) and rise-time (F) for control (white bars) *versus* >15 min SYM2206 (black bars). Inserts are cumulative probability plots comparing the pooled control (thin lines) and SYM2206 data (bold lines) for the respective frequency histograms. Cumulative distributions of amplitude, decay-time and rise-time between control and SYM2206 treatment are significantly different ($p<0.001$ by Kolmogorov-Smirnov and Mann-Whitney tests).

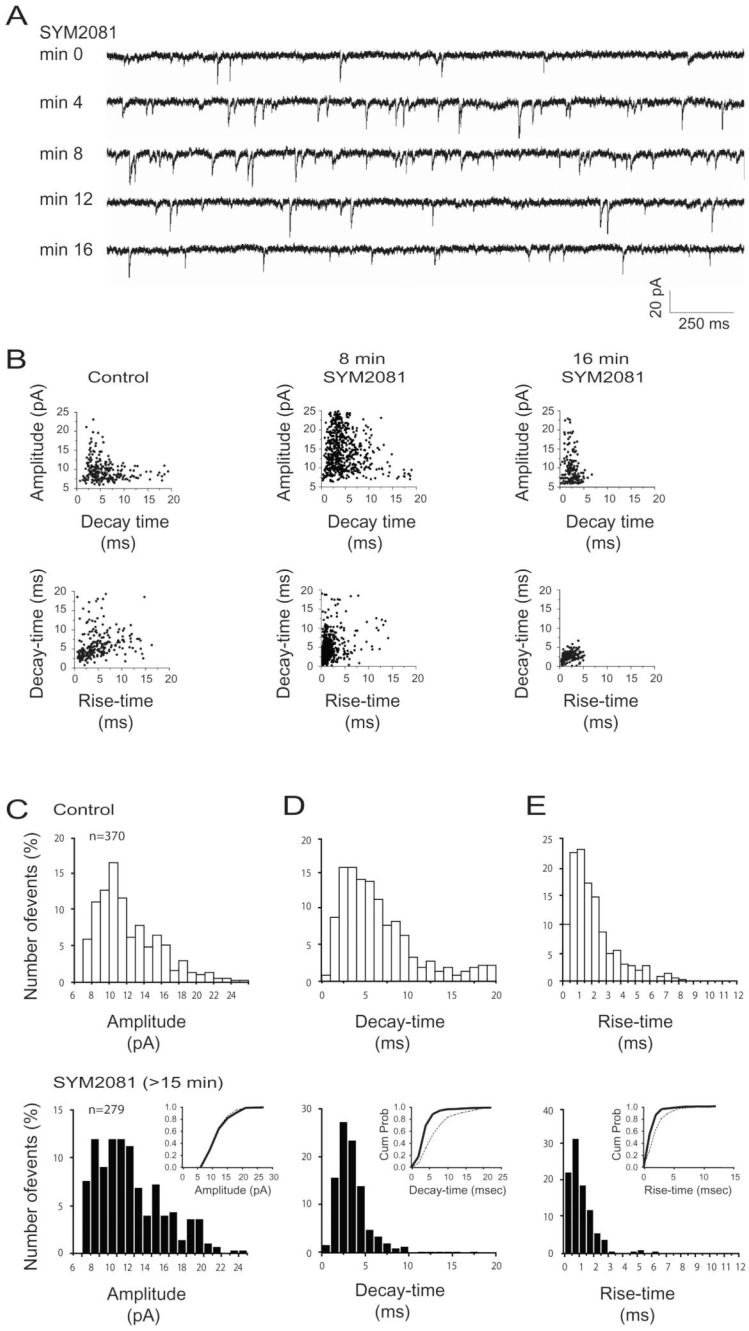

Figure 4.

The slower non-NMDARs mEPSCs can be abolished by long application of SYM2081 to desensitize KARs. A: Representative traces show miniature non-NMDARcs recorded at 7 days AEO. Neurons were held at −70 mV and were perfused with SYM2081 (50 μm). After 4–5 min exposure to SYM2081, the frequency of slow, small miniature currents increased consistent with SYM2081□s agonist properties on KARs. After longer exposure of SYM2081, currents with slower decay- and rise -times disappeared, leaving currents with faster kinetics. B: Scatter plots of a representative neuron showing amplitude *versus* decay-time (upper row) and decay-time *versus* rise-time (lower row) of all miniature non-NMDARcs recorded for 3 minutes under control conditions (left panels), after 8 min

(middle panels), and after 15 min (right panels) of SYM2081 exposure. C–E: Summary frequency histograms from the pooled data of all 4 neurons studied showing the parameters amplitude (D), decay-time (E) and rise-time (F) for control (white bars) *versus* >15 min SYM2081 (black bars) when most KARcs are desensitized. Inserts are cumulative probability plots comparing the pooled control (thin lines) and SYM2081 data (bold lines) for the respective frequency histograms. Cumulative distributions of decay-time and rise-time between control and SYM2081 treatment are significantly different ($p<0.001$ by Kolmogorov-Smirnov and Mann-Whitney tests). Amplitude distribution is not significantly different ($p=0.085$), probably because the slower and smaller KARcs add relatively little amplitude to the AMPAR peak currents when both contribute to the same miniature event and the total number of events recorded is significantly smaller than the number of events recorded in Fig. 3D.

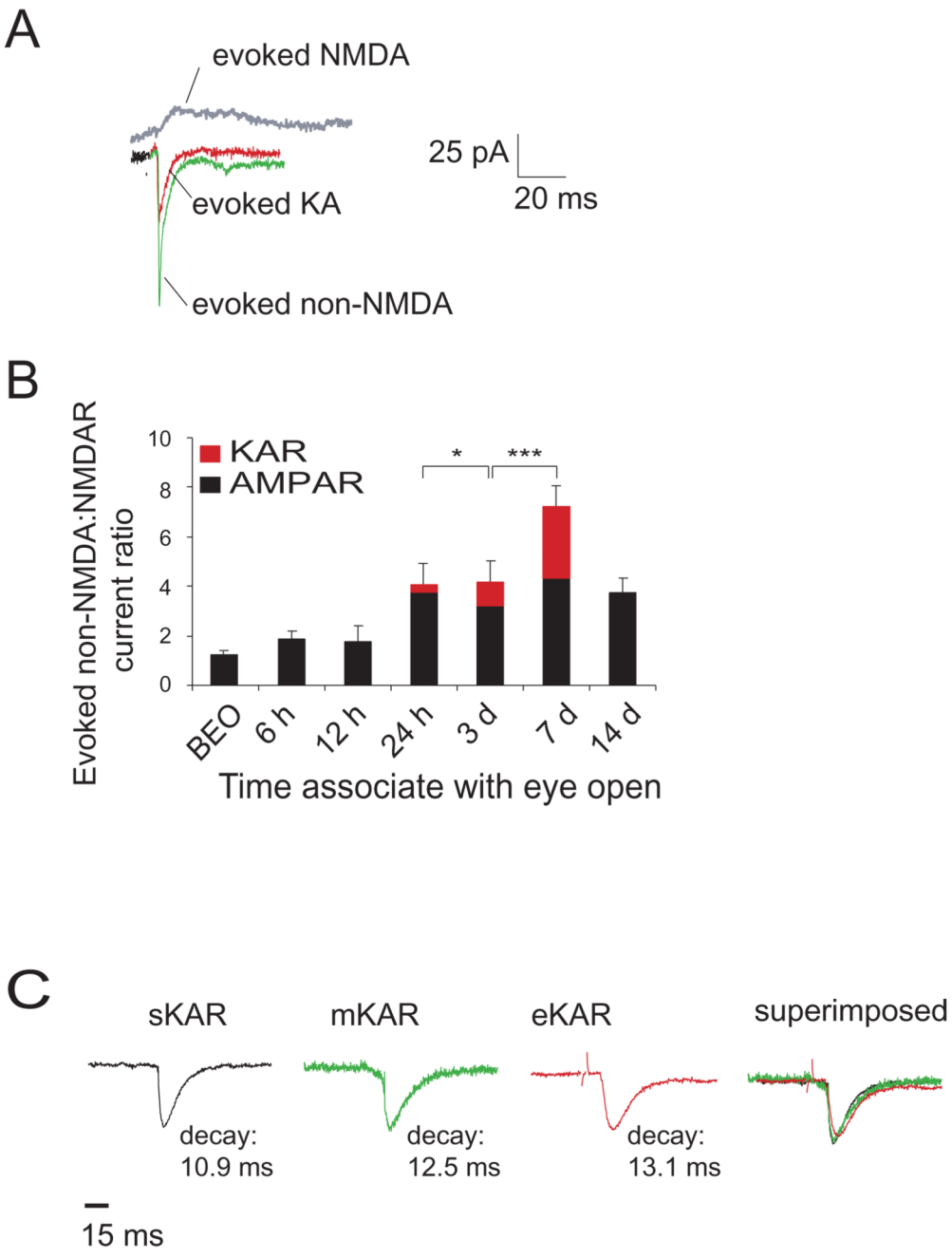

Figure 5.

The contribution of the KARcs relative to non-NMDARcs from 1 to 7 days AEO. A: Traces showing average currents evoked by electrical stimulation of the stratum opticum at +40 mV in Mg^{2+}-containing ACSF with DNQX and BMI to isolate the NMDAR-mediated component (grey line). Non-NMDAR excitatory currents were recorded at −70 mV with APV and BMI (green line). The evoked KARc (red line) was isolated by adding, the AMPAR antagonist SYM2206 (40 μm) to the non-NMDARc bath. B: A histogram showing developmental changes in the contribution of the evoked KARc (red bars) to the total non-NMDAR current (black + red bars) BEO and AEO (n=5–8 neurons per age). Note that the contribution of KARcs relative to non-NMDAR/NMDAR current ratio is evident at 3 to 7

days AEO, but then completely disappears. The black regions of each bar represent the AMPAR contribution which does not change between 1 day and 14 days AEO C: Samples of average spontaneous (black line), miniature (green line) and evoked (red line) KARcs. After rescaling KARcs show similar kinetics for all observed recordings.

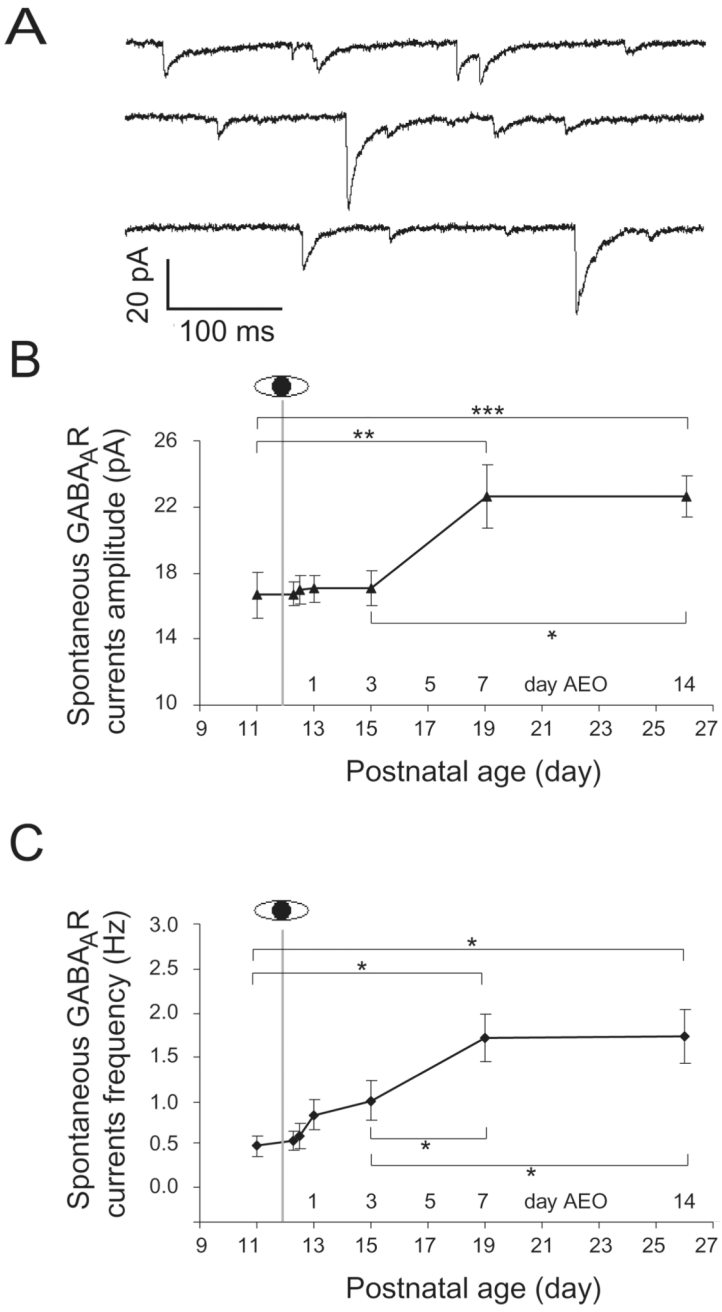

Figure 6.

Increased GABAergic transmission occur between 3 to 7 days AEO. A: Representative traces of spontaneous $GABA_A$Rcs recorded from a sSC neuron at 7 days AEO. The bath solution contained DNQX, $MgCl_2$, and D-APV. Neurons were held at −70 mV below the chloride equilibrium potential. B–C: Summary of quantitative changes in spontaneous $GABA_A$Rc amplitude (B) and frequency (C) relative to the time AEO at P12. The $GABA_A$Rcs increase between 3 and 7 days AEO and remain stable for at least another week. Each symbol represents mean ± S.E.M. obtained from 11–13 neurons. For clarity, significance for the statistical data is shown only for the two closest and most important time points. For more details see Suppl. Table 5 (Fig. 6B) and Suppl. Table 6 (Fig. 6C).